Coherent Processing of Long Series of SAR Images

Francesco De Zan and Fabio Rocca

Dipartimento di Elettronica e Informazione

Politecnico di Milano

20133 Milan, Italy

Email: dezan@elet.polimi.it

Abstract— In the past years, PS analysis has shown its capability to treat simultaneously long series of SAR data. In this contribution an attempt is made to overcome some of the limitations of the said technique, namely its negligence of decorrelation phenomena; a maximum likelihood estimator for the physical parameters of interest is described and some results are presented.

I. INTRODUCTION

During the past decade the availability of long series of coherent SAR images led to the development of multiple-image processing techniques. The advantages of such joint analyses over convetional DInSAR are an increased capability in distinguishing the various contributions to the interferometric phase and consequently a better estimate of atmospheric delay variations, one of the most severe limitations to accurate ground deformation recovery.

We refer in particular to the PS technique [1], which has proven very effective in identifying stable scatterers, with respect to their phase properties, expecially over urbanized areas. The PS technique, in its stricter version, requires the target to possess some well defined geometrical and temporal characteristics: its cross-range extension must be limited and its reflectivity should not change over the entire data set time span. When these requirements are not met by the radar target, the estimates of physical parameters on it are considered unreliable and the point discarded.

Different ways to overcome this limitation have already been proposed. With respect to temporal decorrelation we recall for instance the "Semi-PS/Temporary-PS" concept [2], tackling the case in which a target appears or disappears at some point in the amplitude time series (e.g. when a new building is contructed). Moreover, it is common practice to discard images because of their time isolation or because they represent areas temporary covered by snow (such as winter images in the Alps), since they have no or little chance to be coherent with the main bunch of the data set.

With respect to geometric decorrelation we recall the SBAS technique which carries out the analysis only on small baseline subsets [3] and the so called "higher order interferometry" [4] which models the presence of two dominant scatterers in the resolution cell (with different cross-range positions).

In this paper we present a new attempt of overcoming the above mentioned limitations of standard PS interferometry. The goal is to complete successful estimations of the parameters of interest on a larger number of points. In Section II

the expression of a Maximum Likelihood estimator is derived from a statistical characterization of SAR observables and real data results are presented. Eventually, some considerations are made on the underlying mechanisms of the proposed estimator and on its proximity to standard PS analysis.

II. MAXIMUM LIKELIHOOD ESTIMATOR

A. General Framework

In the following we assume to have N_i SAR images finely coregistered on a common reference called *master*, as usual. We also assume to have already successfully completed a standard PS analysis on the given data set. After compensation for the estimated atmospheric delay (a by-product of the PS analysis) and for the fringes of a reference DEM, the expression of the differential phase with respect to the master and a reference point is as follows (assuming a constant velocity model):

$$\varphi_n = -\frac{4\pi t_n}{\lambda} v - \frac{4\pi B_n}{\lambda \sin \vartheta_0 R} h \qquad (1)$$

In (1) n represents the image number ($1 \leq n \leq N_i$), λ the transmitted wavelength, t_n and B_n the temporal and normal baseline respectively, v and h the target LOS velocity and fine elevation, R is the sensor-target distance and ϑ_0 the local incidence angle (for flat terrain).

If s_n are the N_i complex observations (one for each image), the estimation of h and v through standard PS analysis is given by the maximization of the so called temporal coherence

$$\Gamma(h,v) = \frac{1}{N_i} \left| \sum_{n=1}^{N_i} s_n \exp\left(-j\varphi_n(h,v)\right) \right| \qquad (2)$$

In this case all acquisitions s_n are treated the same, i.e. data are supposed to be affected by the same noise power. In order to take into account their mutual statistical dependences we introduce their covariance matrix

$$C_s = \mathrm{E}[\underline{s}\, \underline{s}^H] \qquad (3)$$

being $\underline{s} = [s_1 \quad s_2 \quad \cdots \quad s_{N_i}]^T$ the vector collecting the N_i observables. The generic element of the covariance matrix can be written as

$$C_s(n,k) = \sigma_n \sigma_k \, \gamma(n,k) \, \exp(j\varphi_n(h,v) - j\varphi_k(h,v)) \quad (4)$$

again supposing a constant velocity model. In (4) σ_n is the standard deviation of the considered target reflectivity in the n-th image and $\gamma(n,k)$ is the real-valued normalized correlation

between pixel s_n and pixel s_k. We rely on the model (1) to fully explain the phase term in (4).

At this point we have developed almost all we need to introduce the Maximum Likelihood (ML) estimator of h and s given the obervations $\underline{s}$ and their covariance matrix C_s. Under the hypothesis of joint gaussian distribution the *pdf* of $\underline{s}$ can be written as

$$f(\underline{s}) = \frac{\exp(-\underline{s}^H C_s^{-1} \underline{s})}{\det(C_s)\, \pi^{N_i}} \tag{5}$$

and the ML estimator can be shown to be

$$[\hat{h}, \hat{v}] = \operatorname{argmin}\left[\underline{s}^H C_s(h,v)^{-1} \underline{s}\right] \tag{6}$$

since $\det(C_s)$ does not depend on h or v. Moreover one can show that it is not necessary to perform a matrix inversion for every choice of h and v but one single inversion is sufficient.

B. Correlation Estimates

Before evalutating expression (6) one should be able to fill the matrix C_s with the correlation $\gamma(n,k)$ between any couple of images, as shown in (4). In order to do that, one can take the absolute value of the sample correlation evaluated over a patch P around the pixel of interest:

$$\hat{\gamma}(n,k) = \frac{\left|\sum_{i \in P} s_n(i) s_k^H(i)\right|}{\sqrt{\sum_{i \in P} |s_n(i)|^2 \sum_{i \in P} |s_k(i)|^2}} \tag{7}$$

An example of correlation matrix is given in Fig. 1.

This estimator is known to be biased and some unbiasing procedure might be useful when dealing with small patches. Some hint on unbiasing is given in [5]. Actually parameter estimation could be carried out also using a complex covariance matrix, simply avoiding taking the absolute value in (7). In that case, however, the resulting $\hat{h}$ and $\hat{v}$ would be referred (intuitively) to the mean behaviour of the averaged pixels in patch P. Moving from estimating h and v towards phase unwrapping one should address the problem of referring the said mean behaviour of the patch to a unique reference in the scene, to obtain an image-scale consistent unwrapping.
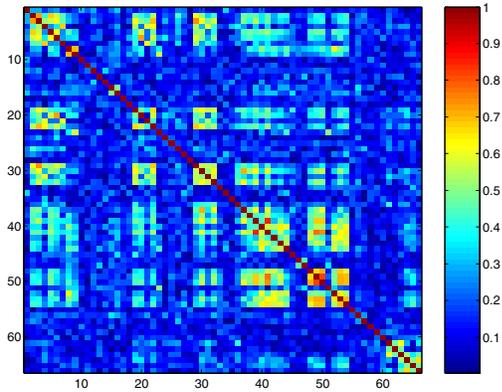

Fig. 1. Sample correlation matrix for 66 ERS scenes

Another way to fill the correlation matrix would be to employ a model for decorrelation. We have analysed different

data sets in the attempt to find some simple decorrelation law as a function of temporal and normal baseline, but preliminary results show that local dynamics are difficult to model with general laws and direct estimates of correlation from the observations seem to be the best choice.

C. Results

We present here some results obtained with the proposed technique on images acquired over the Etna volcano in Sicily. Fig. 2 represents velocity field estimates of an area called Valle del Bove. Common to conventional DInSAR analysis the velocity is relative to some point chosen as a reference. The image on the left shows results obtained maximizing temporal coherence (2), the one on the right those obtained maximizing the likelihood function (6).
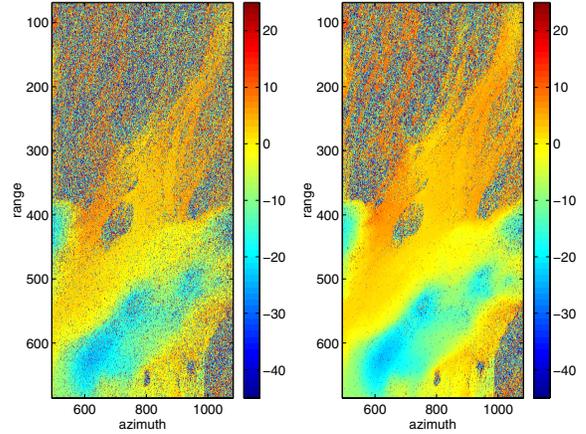

Fig. 2. Comparison of velocity fields obtained maximizing the temporal coherence (left) and the likelihood (right). The color scale reads mm/year.

It is apparent that the latter is more robust. Not only the number of points yielding information is increased, but entire areas that were considered unreliable can now give their contribution. At the same time where both techniques give reliable results, the agreement between them is good.
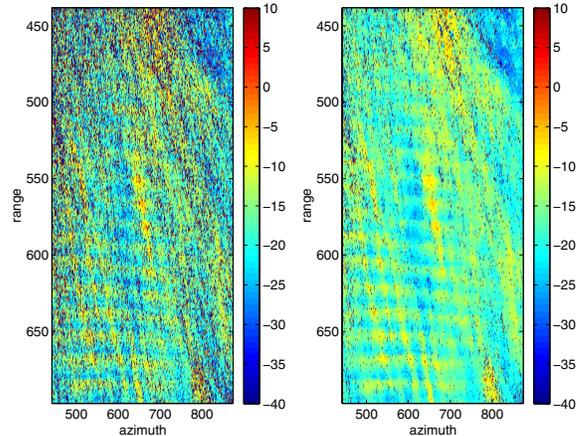

Fig. 3. Comparison of DEM errors estimated maximizing the temporal coherence (left) and the likelihood (right). The DEM error is is given in meters.

The following figure (Fig. 3) shows results obtained with a different dataset (descending orbits) but still on the same region around Etna. Here the comparison is with DEM error estimates. The clearly visible horizontal pattern is possibly due either to SRTM data or to our interpolation routines. Anyway the use of the ML approach gives better results.

D. Eigenvector structure

The inspection of the eigenvectors of the correlation matrix gives some hint on the mechanisms of the ML estimator. If $\underline{\chi}_i$ and λ_i are respectively the eigenvectors and eigenvalues of matrix $C_s(0,0)$ and $\Phi(h,v) = \mathrm{diag}[-\exp(j\varphi_n)]$ then an alternative form of (6) is

$$[\hat{h}, \hat{v}] = \mathrm{argmin} \sum_i \frac{1}{\lambda_i} \left| \underline{\chi}_i^T \cdot \Phi(h,v)\underline{s} \right|^2 \qquad (8)$$

The term $\Phi(h,v)\underline{s}$ is the supposed reflectivity for every choice of h and v, and the estimator picks up the one conforming the most to the expected correlation. In particular a significant portion of energy should be explained with the eigenvectors associated with the highest eigenvalues. An example of eigenvector is given in Fig. 4. It is the first[1] eigenvector of the matrix shown in Fig. 1. It is clear that it reflects the block
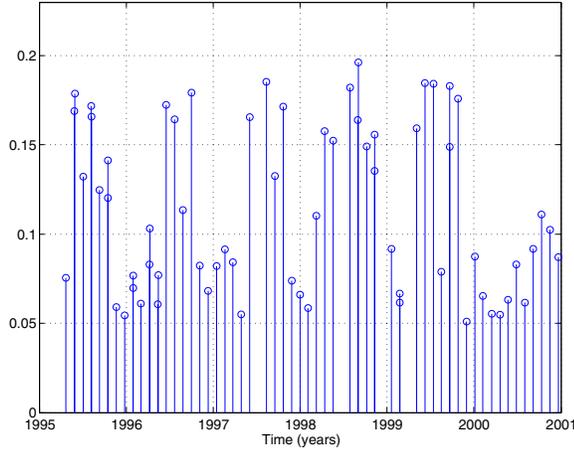

Fig. 4. First eigenvector of sample correlation matrix of Fig. 1

structure of the matrix and could be a good candidate for automatic clustering of snow-free images. Actually it seems to indicate that we should be content with explaining the phases of summer images and shouldn't bother too much with winter images.

Another way to examine correlation values is to sort the matrix indices according to the normal baseline, which is precisely what Fig. 5 and Fig. 6 represent. When the spectral shift is the only source of decorrelation, different takes are correlated according to the well-known triangle law (coherence decreases linearly from 1 to 0 as the normal baseline goes from 0 to the critical baseline). In this case the baseline sampled process is stationary with a mainly low-pass power spectrum,

[1]We assume eigenvectors to be ordered with decreasing magnitude, i.e. $\lambda_1 \geq \lambda_2 \geq \cdots \geq \lambda_{N_i}$.
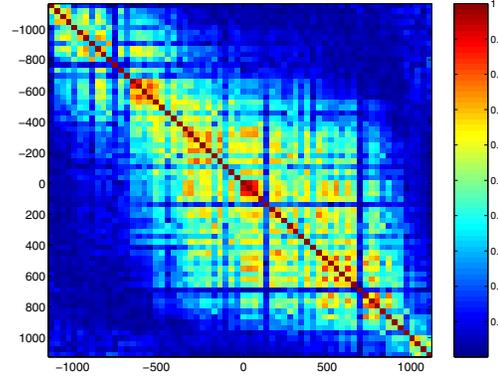

Fig. 5. Sample correlation matrix sorted by normal baseline (meters). Please note that this is a different example from the one in Fig. 1
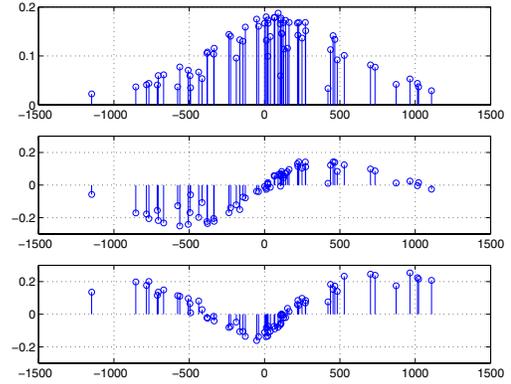

Fig. 6. The first three eigenvectors taken from the sample matrix in Fig. 5 sorted by normal baseline (meters)

namely a squared sinc in the Fourier baseline conjugate domain. The same smoothness or low-pass character can be seen in the strongest eigenvectors. For comparison we give also the theoretical correlation matrix and its first eigenvectors in Fig. 7 and 8.
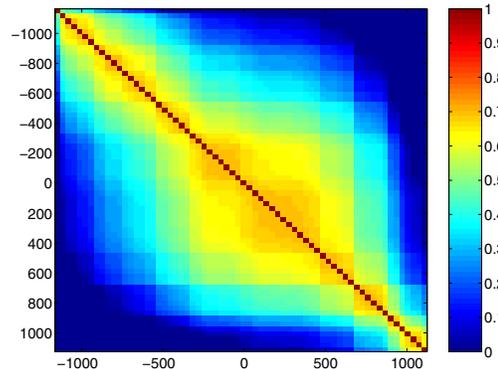

Fig. 7. Expected correlation matrix according to spectral shift theory sorted by normal baseline (meters). We have supposed a coherence of 0.7.

When the correlation between each couple of images is supposed to be the same, the ML estimator in (6) and the one in (2) become exactly the same. This would be the case if
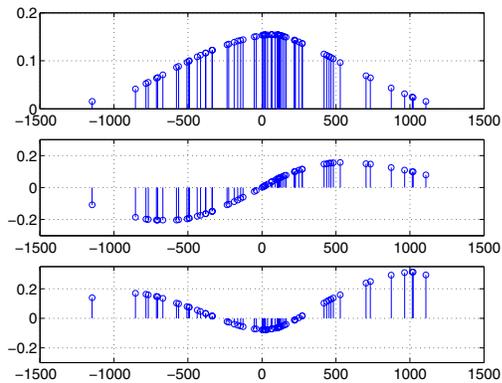
Fig. 8. The first three eigenvectors taken from the matrix in Fig. 7 sorted by normal baseline (meters)

just thermal decorrelation was considered. For instance with a SNR of about 10dB one would obtain

$$\gamma(n,k) = \delta(n-k) + [1 - \delta(n-k)] * 0.9 \qquad (9)$$

III. CONCLUSION

We have proposed a new tool to estimate typical PS parameters from a series of coherent SAR images. Better results are achieved by carefully weighting each image contribution by the means of the sample covariance matrix. Future research efforts should be directed to possibly reducing the sampling of the covariance matrix throughout the scene and to extending the idea to an earlier stage of PS analysis.

ACKNOWLEDGMENT

REFERENCES

[1] A. Ferretti, C. Prati and F. Rocca, "Permanent scatterers in SAR interferometry," *IEEE Trans. Geosci. Remote Sensing*, vol. 39, pp. 8-20, January 2001.

[2] A. Ferretti, C. Colesanti, D. Perissin, C. Prati and F. Rocca, "Evaluating the effect of the observation time on the distribution of SAR Permanent Scatterers," *Fringe 2003*, Frascati, 1-5 December 2003.

[3] R. Lanari, O. Mora, M. Manunta, J. J. Mallorquí, P. Berardino, and E. Sansosti, "A Small-Baseline Approach for Investigating Deformations on Full-Resolution Differential SAR Interferograms," *IEEE Trans. Geosci. Remote Sensing*, vol. 42, pp. 1377-1386, July 2004.

[4] A. Ferretti, M. Bianchi, C. Prati and F. Rocca, "Higher Order Permanent Scatterers Analysis," submitted to *EURASIP Journal On Applied Signal Processing*.

[5] H.A. Zebker and K. Chen, "Accurate Estimation of Correlation in InSAR Observations," accepted for publication in *IEEE Geosci. Remote Sensing Letters*.

[6] R. Everson and S. Roberts, "Inferring the Eigenvalues of Covariance Matrices from Limited, Noisy Data," *IEEE Trans. Signal Processing*, vol. 48, pp. 2083-2091, July 2000.